Scale-up modelling and life cycle assessment of electrochemical oxidation in wastewater treatment

Sara Feijoo[1,*], Sofía Estévez[2], Mohammadreza Kamali[1], Raf Dewil[1,3], and María Teresa Moreira[2]

[1] KU Leuven, Department of Chemical Engineering, Process and Environmental Technology Lab, 2860 Sint-Katelijne-Waver, Belgium
[2] Universidade de Santiago de Compostela, Department of Chemical Engineering, CRETUS, 15782 Santiago de Compostela, Spain
[3] University of Oxford, Department of Engineering Science, Parks Road, Oxford, OX1 3PJ, United Kingdom
* Corresponding author: Sara Feijoo, sara.feijoomoreira@kuleuven.be

Keywords— Electrochemical Advanced Oxidation Processes (eAOPs), Life Cycle Assessment (LCA), wastewater treatment, scale-up modelling, micropollutants

Abstract

The need to improve current wastewater treatments to ensure a clean and sustainable water supply is an unquestionable contemporary challenge. It is therefore essential to facilitate knowledge transfer between research institutions and the industry by developing novel technologies to a proof-of-concept stage, demonstrating both treatment efficiency and compliance with environmental criteria. This study has combined process modelling for the design of an electrochemical Advanced Oxidation Process (eAOP) to remove carbamazepine (CBZ) from wastewater with the identification of the environmental impacts associated with its operation. A comprehensive set of scenarios considering several reactor designs and operating conditions provides the assessment framework to identify the influence of different process variables on the environmental profile of the pilot-scale eAOP. The most sustainable treatment corresponds to the operation of a standardised modular reactor in batch mode, especially when the wastewater has a low concentration of scavengers, such as other ions, organics or pollutants. Nevertheless, in all scenarios evaluated, the main environmental hotspot was attributed to the electrical energy consumed by the auxiliary pumps rather than the electrochemical reactor itself. In comparison to other AOPs, our system showed considerably lower impacts in the global warming potential (GWP) category, with a minimum of 7.6 kg CO_2 eq per g CBZ removed for the most promising scenario. This demonstrates the implementation potential of eAOPs as well as the importance of data from scaled-up experiments, where optimisation should focus on mitigating the impacts of energy-intensive pieces of equipment.

Abbreviations: *API* – Active pharmaceutical ingredient, *B* – Batch mode, *BDD* – Boron-doped diamond, *C* – Continuous mode / Chemical, *CBZ* – Carbamazepine, *CECs* – Contaminant(s) of emerging concern, *COD* – Chemical oxygen demand, *CSTR* – Continuous stirred tank reactor, *E* – Energy, *eAOP(s)* – Electrochemical advanced oxidation process(es), *EC* – Enhanced conductivity, *FB* – Fed-batch mode, *FE* – Freshwater eutrophication, *FRS* – Fossil resource scarcity, *FU* – Functional unit, *GAC* – Granular activated carbon, *GWP* – Global warming potential, *H* – High content, *L* – Low content, *LCA* – Life cycle assessment, *M* – Multicomponent, *ME* – Marine eutrophication, *NF* – Nanofiltration, *RL* – Regulatory limits, *SDG* – Sustainable development goal, *SPF* – Solar photo-Fenton, *SW* – Synthetic wastewater, *TA* – Terrestrial acidification, *TET* – Terrestrial ecotoxicity.

1 Introduction

In 2020, approximately 2 billion people lacked safely managed drinking water, 2.3 billion people suffered from poor hygiene and up to 3.6 billion people did not have access to basic sanitation, which has raised some concern about the accomplishment of Sustainable Development Goal (SDG) No. 6 on Clean Water and Sanitation by 2030 [1]. One of the root causes is the occurrence of contaminants of emerging concern (CECs) in wastewater treatment plant effluents, which represents a major issue not only to human health but also to ecosystems [2–5]. Carbamazepine (CBZ) is one of these contaminants since it is a pharmaceutical poorly removed by conventional biological treatment (i.e., removal efficiency is typically lower than 10%) [6–8]. In fact, due to its widespread consumption and recalcitrant nature, CBZ has been recently found to be the most recurring active pharmaceutical ingredient (API) in river basins worldwide [9].

One of the solutions to this problem is the development novel wastewater treatments that prevent the release of pollutants through their effective degradation, as is the case of Advanced Oxidation Processes (AOPs). AOPs are an extensive family of treatments comprising ozonation, heterogeneous and homogeneous (photo)catalysis, Fenton and Fenton-like processes, and electrochemical-, ultrasound-, microwave- or gamma-radiation treatments as well as any of their combinations [10]. Among these various technologies, electrochemical Advanced Oxidation Processes (eAOPs) have received significant attention in recent years [11–13]. They are commonly used as tertiary wastewater treatments, driving pollutant degradation through direct and indirect oxidation pathways by electrochemically generating highly reactive oxidative species, mainly hydroxyl ($^{\cdot}OH$) and sulfate ($SO_4^{\cdot-}$) radicals [14–16]. Electrochemical AOPs allow for high degradation efficiencies and reaction rates under mild conditions, while showing no or limited dependence on chemical addition [2, 17]. Other advantages are their versatility, ease of process integration and safe operation [13, 18].

When implementing an eAOP, the selection of the electrode material and the precursor species for the oxidative radicals are key factors influencing the overall treatment efficiency and selectivity [14]. Boron-doped diamond (BDD) electrodes are of particular interest for wastewater applications, as they have demonstrated high efficiency in the generation of oxidative species and degradation of several contaminants, as well as high conductivity, stability, O_2 overpotential and durability [17, 19, 20]. Despite the significant energy consumption associated with electrochemical treatments [15], the in situ radical generation offered by the BDD material from water molecules [21] and ionic species such as sulfate ions [22, 23] has a high added value for industrial implementation, given that they are already available in wastewater streams [24, 25]. The absence of additional chemicals can minimise not only the overall consumption of raw materials but also the generation of secondary waste streams and hence the associated environmental impacts [10]. Consequently, achieving SDG No. 6 while aiming for sustainable and carbon neutral processes is essential to provide a far-reaching solution. In this regard, the Life Cycle Assessment (LCA) methodology is a useful resource for evaluating the environmental friendliness of novel eAOPs. Nonetheless, as of June 2022, a Scopus search for studies applying LCA methodology to electrochemical oxidation in wastewater treatment retrieved 281 documents, of which only 8 publications specifically included an electro-oxidation system (Table C.1). Among these studies, none were dedicated to the removal of pharmaceuticals, 5 were applied to synthetic or real wastewater matrices, and

only two considered wastewater volumes at a large scale. Consequently, there is a significant knowledge gap on the environmental implications of eAOPs in wastewater treatment.

In our previous work [26], two preliminary design considerations for the implementation of a BDD-based eAOP as a tertiary wastewater treatment were addressed: the effects of the wastewater composition and the reactor mode of operation. A comparative assessment of 8 different scenarios, both in terms of CBZ degradation and electrical energy consumption per unit of effective operation time, revealed that the competition reactions taking place due to wastewater components could be mitigated when operating in fed-batch mode, since a 2.1-fold increase in CBZ degradation and a 60% reduction in energy consumption were achieved with respect to a conventional batch operation. Similarly, operating in continuous rather than batch mode resulted in significant energy savings (approximately 19%) for similar degradation efficiency. However, in order to further evaluate the advantages and disadvantages of each of the investigated scenarios, it is essential to take into account their potential environmental impact when applied on a larger scale. In fact, most conventional municipal wastewater treatment plants already involve high energy consumption from the grid due to all the machinery involved [27], leading to a significant carbon footprint (i.e., 23–432 kg CO_2 per population equivalent) [27–29], of which approximately 70% was attributed to the indirect emissions from energy requirements [29].

To fill the knowledge gap on the environmental performance of pilot-scale eAOPs for the removal of pharmaceuticals from secondary wastewater effluents, this study focused on conducting a techno-environmental analysis including the following:

(i) Development of a scale-up model to translate the laboratory results into a pilot-scale operation. To this end, two reactor configurations have been considered: a standardised modular reactor and a vertical plate stirred tank reactor.

(ii) Quantification of the environmental profile of the eAOP by LCA methodology under multiple experimental conditions. More specifically, the influence of the reactor configuration, the mode of operation (namely, batch, fed-batch and continuous), the wastewater matrix (considering various compositions of pure and synthetic wastewater, different amounts of oxidising species and the possible presence of additional pollutants) and the potential oversizing effect have been evaluated.

2 Methodology

2.1 Experimental scenarios

The micropollutant degradation experiments were carried out using a BDD electro-oxidation system, as previously described by Feijoo et al. (2022) [26]. Both single and multicomponent systems were primarily aimed at CBZ removal, where a diverse set of concentrations for oxidative and scavenger species were investigated. The reactor operating modes included in the comparative analysis were batch, fed-batch and continuous. As a result, the following 8 scenarios were evaluated in the techno-environmental analysis:

- Scenario of “Regulatory Limits for Sulfates and Nitrates Conducted in Batch Mode (RL-B)”: CBZ degradation was carried out in batch mode and in a pure water matrix containing the concentration limits for nitrate (50 mg/L) and sulfate (250 mg/L) ions as defined by their respective EU directives [30, 31].

- Scenario of “Enhanced Conductivity Medium Conducted in Batch Mode (EC-B)”: an extension of the RL-B scenario assumed that nitrate and sulfate concentrations were higher than the regulatory limits, at 100 mg/L and 500 mg/L, respectively.

- Scenario of “Enhanced Conductivity Medium in Synthetic Wastewater with Low Organic Load Conducted in Batch Mode (ECSWL-B)”: CBZ degradation was performed in batch mode and in the presence of the enhanced nitrate and sulfate concentrations as in the EC-B scenario. The treated water matrix consisted of a synthetic secondary effluent with low concentrations of other organics and ions (COD: 25.2 mg/L, total N: 5.0 mg/L, total P: 0.5 mg/L, alkalinity: 2.5 mg/L).

- Scenario of “Enhanced Conductivity Medium in Synthetic Wastewater with Higher Organic Load Conducted in Batch Mode (ECSWH-B)”: this variation to the ECSWL-B scenario consisted of the degradation of CBZ in a synthetic wastewater matrix with a high ion and organic composition (COD: 50.4 mg/L, Total N: 10.0 mg/L, Total P: 0.9 mg/L, Alkalinity: 4.9 mg/L).

- Scenario of “Enhanced Conductivity Medium in Synthetic Wastewater with Low Organic Load Conducted in Fed-Batch Mode (ECSWL-FB)”: this modification to the ECSWL-B scenario consisted of fed-batch operation, where CBZ spikes were added at the beginning of each 60 min cycle for a total of 6 cycles to reuse sulfate and nitrate species already present in the wastewater.

- Scenario of “Enhanced Conductivity Medium in Synthetic Wastewater with Low Organic Load Conducted in Continuous Mode (ECSWL-C)”: the ECSWL-B was adapted to a continuous operation, that is, with continuous inlet and outlet flows set to 25 mL/min, leading to an average residence time of 30 min.

- Scenario of “Multicomponent System in Synthetic Wastewater with Low Organic Load Conducted in Batch Mode (MSWL-B)”: this variation to the ECSWL-B scenario consisted of the simultaneous degradation of CBZ with additional micropollutants, including caffeine, diclofenac and sulfamethoxazole.

- Scenario of “Multicomponent System in Synthetic Wastewater with Low Organic Load Conducted in Fed-Batch Mode (MSWL-FB)”: this modification to the MSWL-B scenario was conducted in fed-batch mode for 6 cycles of 60 min with multicomponent spikes.

2.2 Selected reactor designs

After conducting a review of available configurations for pilot-scale BDD electrochemical reactors, it was observed that a large number of studies considered commercial DiaCell® units

[32–38], filter press flow cells [38–41], multielectrode stacks with a serpentine array [39–41], or a vertical electrode plate arrangement in a stirred tank reactor [39, 42, 43]. In this study, the two designs selected were (i) a standardised modular reactor inspired by the DiaCell® units and (ii) a fully customised vertical plate stirred tank reactor (Fig. 1). Both configurations are commonly reported in the literature, feasible to scale up and significantly different from each other in terms of area, geometry and distance between the electrodes.

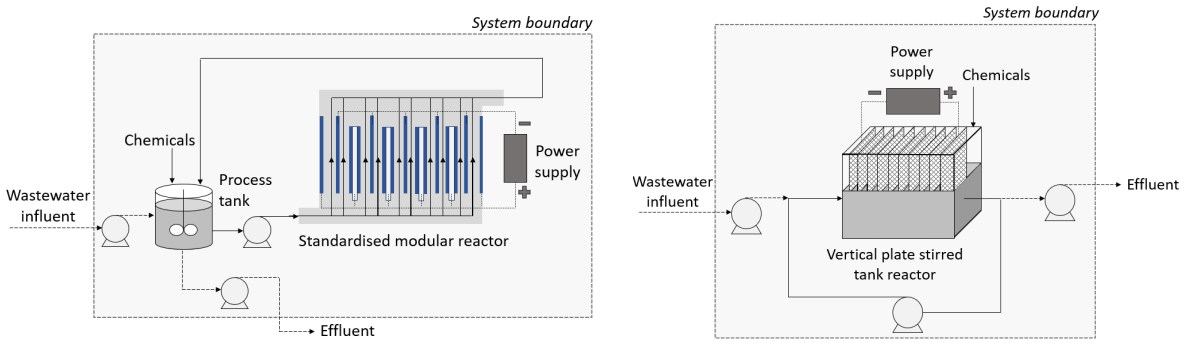

(a) Standardised modular reactor. **(b)** Vertical plate stirred tank reactor.

Figure 1: Schematics of the **(a)** standardised modular reactor and **(b)** vertical plate stirred tank reactor. For their fed-batch operation, a dosing pump is added.

2.2.1 Standardised modular reactor design

The standardised modular reactor configuration was based on the DiaCell® 1001 electrochemical cell [34, 36]. It comprises multiple compartments constituted by two BDD anodes and one stainless steel cathode with an interelectrode distance of 1 mm, leading to a total of 10 anodes and 5 cathodes per cell. Standard shapes for the electrodes are circular, with a surface area of 70 cm^2 and monopolar connections (Fig. 1a). During its operation, a process tank is loaded with the secondary wastewater to be treated, and if needed, additional chemicals are added. Afterwards, the content of the tank is continuously stirred and fed to the standardised modular reactor, where it is distributed between five compartments in parallel. The system operates in recirculation mode, meaning that the total volume of wastewater remains constant and is recirculated until the desired degradation is attained. Consequently, this reactor design is applicable for batch and fed-batch operations. Finally, the treated effluent is accumulated in the process tank and discharged.

2.2.2 Vertical plate stirred tank reactor design

The vertical plate stirred tank reactor consists of a set of parallel monopolar electrodes that are fully immersed in the bulk of the reactor (Fig. 1b). The number of electrode pairs as well as their size and arrangement are versatile parameters, and hence, any reactor design can be implemented. To avoid any damage to the electrodes during operation, stirring inside the reactor is promoted by the inlet and the recirculation pump flows. In addition, the electrode channels can contain an inert polymer mesh and other turbulence promoters to improve mass transfer. It is assumed that the current density and voltage are uniformly distributed across the

cell. This type of setup allows for either a batch, fed-batch or continuous operation with recirculation.

2.3 General scale-up considerations

Based on the collected experimental data from laboratory experiments in a 1 L electrochemical cell, the scale-up target was to model the steady-state conditions in a 100 L reactor filled up to 75% of its capacity and where 90% CBZ degradation can be attained. The scale-up methodology consisted of analysing the experimental results based on the reaction kinetics, electrical consumption and treatment capacity. This enabled mass and energy balances to be performed at the pilot scale, with the required pieces of equipment (i.e., electrochemical cell and associated pumps) designed accordingly. Relevant scale-up considerations are defined in the following subsections.

2.3.1 Common design conditions

To compare scenarios under the same time reference, all reactor designs were simulated to operate for 1 day (i.e., 24 h). The number of batch and fed-batch experiments during that time to achieve 90% removal of CBZ were calculated considering the effective reaction times observed experimentally. In addition, a total of 25 min was considered per experiment to account for preparation, charge and discharge activities.

The starting concentrations of the different chemicals involved were assumed to be the same as in the experiments at the lab scale, given that they are independent of the reactor type and size. Therefore, their total initial mass was directly proportional to the scaled-up reactor volume. For the addition of sulfate and nitrate ions, only the differential concentrations with respect to the regulatory limits were considered as input chemicals in the LCA inventory, given that it is plausible that the regulatory limits may already be found in the influent wastewater. In the case of fed-batch operation, it was assumed that a concentrated stream of 200 mg/L CBZ was used for the spikes to guarantee that volume variations after their addition during 1 day of operation would not yield to more than an overall 10% increase.

2.3.2 Mass balance assumptions

Since the kinetic constants (k, h^{-1}) were determined from lab-scale experiments, a correction factor was applied to estimate the final CBZ concentrations in the pilot-scale standardised modular reactor. The need for a correction factor in this specific reactor configuration arises from the differences in the number of electrodes and subsequent electroactive areas between the lab-scale reactor used and the scaled-up design. These differences lead to distinct area-to-volume ratios, and therefore, the variation in kinetic constants has been estimated accordingly. As shown in Eq. 1, k is related to the mass transfer coefficient (k_m, m/h), a pseudo-first order kinetic constant related to the activity of inorganic oxidants (k_i, h^{-1}), the electroactive area (A, m^2) and the reactor volume (V, m^3) [34, 44]. Assuming that k_i is negligible in our system as oxidants are present in excess and that k_m remains constant with increasing scale, the observed

kinetics are affected by the *A/V* ratio. Consequently, the kinetic rate constants in the batch and fed-batch scaled-up standardised modular reactor (k_{scale}, h^{-1}) were calculated as shown in Eq. 2, where *A* and A_{scale} are the electroactive areas (m^2) at the lab and pilot scales, respectively, and *V* and V_{scale} are the volumes (m^3) of treated wastewater at the lab and pilot scales, respectively.

$$COD = COD_0 \cdot e^{(-k \cdot t)} = COD_0 \cdot e^{\left(-\left(\frac{A}{V} \cdot k_m + k_i\right) \cdot t\right)} \quad (1)$$

$$k_{scale} = k \cdot \frac{A_{scale}/V_{scale}}{A/V} \quad (2)$$

Similarly, the modelling for the continuous operation was based on the definition of an ideal continuous stirred tank reactor (CSTR) (Eq. 3), where *X* is the conversion of the target pollutant obtained experimentally and τ is the residence time (h). After substitution of common terms with Eq. 2, the conversion in the scaled-up standardised modular reactor (X_{scale}) was obtained from Eq. 4, where *F* and F_{scale} are the flow rates (m^3/h) of treated wastewater at the lab and pilot scales, respectively. Given that a target of 90% CBZ removal was selected, Eq. 4 was used to retrieve the required flow rate at the pilot scale [34, 45].

$$k_{CSTR} = \frac{X}{1 - X} \cdot \frac{1}{\tau} \quad (3)$$

$$\frac{X_{scale}}{1 - X_{scale}} = \frac{X}{1 - X} \cdot \frac{A_{scale}/F_{scale}}{A/F} \quad (4)$$

Regarding the vertical plate stirred tank reactor, the experimental kinetic constants were used in the mass balance since the area-to-volume ratio was considered constant. For other wastewater components, it was assumed that they were present in excess and that variations in concentration during the treatment were negligible. In addition, the consumption of NaOH to neutralise acidic outlet streams before discharge was also calculated at the pilot scale and included in the mass balance.

2.3.3 Energy balance assumptions

The limiting current density (j_{lim}, A/m^2) of each treatment was estimated based on the model developed by Panizza et al. (2001) defined in Eq. 5, where *F* is the Faraday constant (C/mol), k_m is the average mass transport coefficient in the electrochemical cell (m/s) and *COD* is the chemical oxygen demand expressed in mol O_2/m^3 [46]. The mass transport coefficient (k_m) at the pilot scale was estimated according to the correlations as a function of the flow rate proposed by Anglada et al. (2009) [47], with a maximum value of approximately $1.7 \cdot 10^{-5}$ m/s for a 10 L/min flow.

$$j_{lim} = 4 \cdot F \cdot k_m \cdot COD \quad (5)$$

As a result, scenarios involving wastewater with low and high concentrations of organics and

other ionic species showed estimated limiting current densities of 5.2 and 10.3 A/m^2, respectively. Given that experiments were performed at higher current densities, it can be concluded that electrochemical oxidation is under mass transport control and that pollutant and COD removal follow an exponential trend.

The electrical energy consumption by the pilot-scale pumps (P_{pump}, kWh), which depends on the supplier catalogue nominal power (P_n), was determined based on the modelled operation time (t, h), as shown in Eq. 6. The operation time for the recirculation, inlet and outlet pumps corresponded to the actual reactor operation, whereas for the pumps dedicated to individual charge, discharge and dosing operations, it was calculated as the time required to transport a scaled-up volume of liquid (V_{scale}, m^3) at a specific flow rate (F_{scale}, m^3/h), as shown in Eq. 7.

$$P_{pump} = P_n \cdot t \tag{6}$$

$$t = \frac{V_{scale}}{F_{scale}} \tag{7}$$

For batch and fed-batch operations in both reactor configurations, centrifugal pumps used for charge/discharge operations were assumed to be similar to the model KPM 50 by Speroni S.p.A., which has a P_n of 0.37 kW and can operate between 5 and 30 L/min [48]. The selected flow rate for the charge/discharge pumps was 15 L/min to minimise time losses during the 1-day operation. During the electrochemical treatment, the same pump type was considered in both reactors to drive a continuous recirculation at 10 L/min to ensure a Reynolds number higher than 500 [49].

The dosing pump for the fed-batch operation in both reactor configurations was assumed to be similar to the Model A peristaltic pump by Redox.me, which has a P_n of 0.04 kW and can operate between 0.07 and 380 mL/min [50]. The selected flow rate was approximately 5 mL/min.

For continuous operation, which is only applicable to the vertical plate stirred tank reactor, model KPM 50 was also selected for the recirculation pump, whereas the WT600F-65/KZ25 model by Golander Pump was chosen as the inlet/outlet pump, with a P_n of 0.2 kW and a flow rate window between 0.25 and 6 L/min [51]. The selection of these pumps is justified based on an in-depth analysis regarding the scaled-up flow rates needed, since the flow rate directly influences the mass transfer and the residence time inside the reactor, and hence, the overall conversion and the electrical energy consumption. Given that it was desired to ensure a recirculation flow rate with a Reynolds higher than 500, an approximate recirculation ratio of 10 was required (Fig. A.1a). Based on that ratio, the effect of the selected influent flow rate on the entire electrochemical system was investigated. As depicted in Fig. A.1b, an influent flow rate of 0.75 L/min was required for an overall 90% conversion, meaning that the recirculation flow rate had to be approximately 8.2 L/min. Both these flow rates can be delivered with the selected pumps, and therefore, their catalogue nominal power allowed for a suitable energy estimation.

2.4 LCA framework

2.4.1 Goal and scope

The goal of the Life Cycle Assessment (LCA) study was to evaluate the environmental profile of the pilot-scale electrochemical oxidation of CBZ when several secondary wastewater compositions and reactor configurations were involved. Therefore, attention was paid to the operation stage, and scenarios were evaluated from a gate-to-gate perspective. That is, the operation of the electrochemical reactor and its associated pumps was considered, whereas the impacts related to construction, decommissioning, upstream and downstream processes were excluded. The analysis consisted of an attributional LCA following ISO standards 14040:2006 and 14044:2006 [52, 53].

2.4.2 Assessment method

The LCA was performed using the ReCiPe MidPoint (H) V1.06/World (2010) and EndPoint (H/H) V1.06/World (2010) methods [54] in SimaPro 9.3.0.2. software [55]. The following impact categories were selected as they are representative of energy, toxicity and water effects: global warming potential (GWP), terrestrial acidification (TA), freshwater eutrophication (FE), marine eutrophication (ME), terrestrial ecotoxicity (TET) and fossil resource scarcity (FRS). Additional results on other impact categories can be found in the Supplementary Material, Appendix B. The functional unit (FU) selected was 1 mg of CBZ removed per cubic metre of wastewater treated during one day of operation, and hence, its units are mg/(m^3·day). Based on the different reactor configurations modelled at the pilot scale and the estimated inventories (Tables A.4 and A.5), the following environmental analyses were conducted:

(i) To elucidate the influence of the reactor operating mode, the results of the scale-up modelling for all experimental scenarios were analysed in terms of chemical and energy requirements per FU in the vertical plate stirred tank reactor. Based on these results, a benchmark on the environmental profiles of the batch, fed-batch and continuous modes was conducted. To this end, the ECSWL-B, ECSWL-FB and ECSWL-C scenarios were compared. The results reported correspond to the midpoint assessment method.

(ii) To discern the effect of the wastewater matrix, a benchmark on the environmental profiles when diverse influent compositions are treated in the standardised modular reactor in batch mode was conducted. To this end, the RL-B, EC-B, ECSWL-B, ECSWH-B and MSWL-B scenarios were compared. The results reported correspond to the midpoint assessment method.

(iii) To determine the influence of the reactor configuration, a benchmark on the environmental profiles of the standardised modular reactor and the vertical plate stirred tank reactor operated in batch mode was conducted. To this end, the RL-B, EC-B, ECSWL-B, ECSWH-B and MSWL-B scenarios were compared for both reactor types. The results reported correspond to the midpoint and endpoint assessment methods.

(iv) The oversizing effect was analysed for the standardised modular reactor. Given that this

reactor configuration is oversized by default due to the impositions of the commercially available cells, an equivalent oversizing factor was applied to the vertical plate stirred tank reactor. The environmental profiles of the different configurations were determined from both midpoint and endpoint perspectives.

3 Results

3.1 Scale-up modelling

3.1.1 Standardised modular reactor for batch and fed-batch systems

The pilot-scale design of the standardised modular reactor was based on the assumption that the anodic area to volume ratio (A/V, m^2/m^3) remains within the same order of magnitude with increasing scale [34]. Based on the standard electrode areas (A_{std}, m^2) for this reactor configuration, the number of anodes (N_a) required for the scaled-up reactor volume (V_{scale}, m^3) was calculated according to Eq. 8. Since standard modular electrochemical cells are made of stacks with 10 anodes per cell ($N_{a/cell}$) [34], N_a was rounded up to the closest multiple of 10 ($N_{a/r}$), and the scaled-up anodic area (A_{scale}) was calculated under Eq. 9. The scaled-up anodic area to volume ratio (A_{scale}/V_{scale}) was recalculated, and a difference of less than 18% was observed.

$$N_a = \frac{A/V \cdot V_{scale}}{A_{std}} \tag{8}$$

$$A_{scale} = A_{std} \cdot N_{a/r} \tag{9}$$

The electrical energy consumed by the electrodes (P_{elec}, kWh) in the standardised modular reactor was calculated as the product of the current applied (I_{scale}, A), the potential difference (V_{diff}, V) and the reaction time (t, h) to achieve 90% CBZ degradation, as shown in Eq. 10, including a 10% excess to account for energy losses due to AC/DC transformations [56]. The current applied at the pilot scale (I_{scale}, A) was estimated from the current density (j, A/m^2) applied experimentally and the calculated pilot-scale anodic area (A_{scale}, m^2) (Eq. 11). The potential difference at the pilot scale (V_{diff}, V) could not be directly extrapolated from the experimental results, given the differences in interelectrode distances between both setups. Therefore, V_{diff} was determined from the lab-scale potential (V_{lab}, V) adjusted with the effective potentials (V_{eff}, V) consumed at the lab and pilot scales (Eq. 12). These effective potentials were calculated based on Ohm's law, as indicated in Eq. 13, where l is the interelectrode distance (m) and K is the conductivity of the wastewater (S/m).

$$P_{elec} = \frac{I_{scale} \cdot V_{diff}}{1000} \cdot t \cdot (1 + 10\%) \tag{10}$$

$$I_{scale} = j \cdot A_{scale} \tag{11}$$

$$V_{diff} = V_{lab} - V_{eff,lab} + V_{eff,scale} \tag{12}$$

$$V_{eff} = \frac{j \cdot l}{K} \quad (13)$$

The electrical energy consumed by the agitation in the process tank was calculated from the power input/volume ratio (P/V, W/m^3) at the lab scale, as shown in Eq. 14. This ratio is assumed to remain constant with the scale-up [57], with a value ranging from 0.5 to 16 kW/m^3 [58]. In the application of Eq. 14, N_p corresponds to the impeller power number (assumed to be 3 for common impellers at high Reynold numbers [59]), ρ is the density of the wastewater (kg/m^3), N is the agitation speed used in the lab experiments (rps), d is the outer diameter of the used impeller (m), and V is the volume of wastewater inside the electrochemical cell (m^3). Therefore, when P/V is calculated for the tested lab conditions, the total agitation power (P_{agit}, kWh) consumed at a larger scale to stir a volume of wastewater (V_{scale}, m^3) for a given period of time (t, h) can be calculated as shown in Eq. 15.

$$P/_V = \frac{N_p \cdot \rho \cdot N^3 \cdot d^5}{V} \quad (14)$$

$$P_{agit} = \frac{P/_V}{1000} \cdot V_{scale} \cdot t \quad (15)$$

A summary of the standardised modular reactor design resulting from the scale-up modelling can be found in Table A.1.

3.1.2 Vertical plate stirred tank reactor for batch, fed-batch and continuous systems

The scale-up of the vertical plate stirred tank reactor was made assuming 15 electrode pairs (p), where the electrode shape was selected to be rectangular plates with a 92 cm^2 surface area [34] and a height to width ratio of 0.3. Consequently, the required height of liquid (h_l, m) was calculated considering that the electrode height (h_e, m) corresponds to a certain reduction (R, %) according to Eq. 16. The length of the reactor (l_r, m) was estimated based on the anode thickness (l_a, m), the cathode thickness (l_c, m) and the interelectrode distance (l, m) with a 10% excess, as shown in Eq. 17. These parameters enabled the calculation of the reactor width (w_r, m) given the scaled-up volume of wastewater to be treated (V_{scale}, m^3) (Eq. 18). Finally, the height of the reactor (h_r, m) was estimated with Eq. 19 based on a geometrical volume (V_T) of 100 m^3.

$$h_l = \frac{h_e}{1 - R} \quad (16)$$

$$l_r = (l_a + l_c + 2 \cdot l) \cdot p + l_a + 2.1 \cdot l \quad (17)$$

$$w_r = \frac{V_{scale}}{h_l \cdot l_r} \quad (18)$$

$$h_r = \frac{V_T}{l_r \cdot w_r} \quad (19)$$

The electrical energy consumed by the electrodes (P_{elec}, kWh) in the vertical plate stirred tank reactor was calculated as shown in Eq. 10. In contrast to the calculations for the standardised modular reactor, the potential difference at the pilot scale (V_{diff}, V) was assumed to be equivalent to the lab-scale measurements since the same interelectrode distance was selected. The current applied to each electrode pair at the pilot scale (I_{scale}, A) was calculated according to Eq. 20, since the electrodes are arranged in parallel, and the current is distributed equally among them.

$$I_{scale} = \frac{j \cdot A_{scale}}{N_a} \tag{20}$$

A summary of the vertical plate stirred tank reactor design resulting from the scale-up modelling can be found in Table A.2.

3.1.3 Scaled-up inventory of chemicals and energy

A summary of the daily treatment capacity for each scenario resulting from the scale-up modelling is provided in Table A.3. Based on these results, an overview of the gate-to-gate chemical and energy requirements in the different reactor designs and modes of operation per FU are depicted in Tables A.4 and A.5.

3.2 Environmental profiles

3.2.1 Benchmark of modes of operation

A preliminary benchmark on modes of operation was conducted based on their chemical and energy consumption in the different scenarios under study. To this end, the inventory for the vertical plate stirred tank reactor (Table A.5) was visualised to enable the comparison. As depicted in Fig. 2, the scenario with the highest chemical consumption corresponded to the continuous operation in ECSWL-C, which is due to the continued addition of sulfate and nitrate species over the concentrations defined by the regulatory limits in the RL-B scenario (i.e., 250 mg/L for sulfate and 50 mg/L for nitrate). Other scenarios operated in batch mode (i.e., EC-B, ECSWL-B, ECSWH-B and MSWL-B) entailed a chemical consumption that was 34-78% lower than the ECSWL-C scenario, depending on whether the wastewater presented a high or low complexity in composition. The fed-batch operation was the mode of operation with the lowest chemical consumption, given that additional nitrate and sulfate were only supplied in the first cycle and were reused for the successive cycles. As a result, fed-batch scenarios consumed 74-93% fewer chemicals than the continuous operation ECSWL-C. Finally, the addition of sodium hydroxide to neutralise acidic effluents was negligible in comparison to other chemicals (i.e., less than 0.002% in all scenarios).

For energy consumption, the opposite trend was observed. The scenarios with the highest energy demand were those operated in fed-batch mode (i.e., MSWL-FB and ECSWL-FB), which primarily corresponded to the operation of the recirculation pump and was particularly increased in a multicomponent wastewater matrix. The reason behind this outstanding

contribution is twofold. First, the fed-batch system presented a lower treatment capacity of wastewater (Table A.3), which is taken into consideration for the definition of the FU and hence for the inventory results. Second, due to the competition kinetics in the multicomponent system, the overall CBZ degradation was negatively affected, which exacerbated the energy demand of the treatment due to increased operation times. The scenarios in batch mode presented a considerably lower energy consumption in comparison to MSWL-FB, being approximately 94-98% lower for those with low wastewater complexities (i.e., RL-B, EC-B and ECSWL-B) and 78-85% otherwise (i.e., ECSWH-B and MSWL-B). The continuous operation had a total energy consumption comparable to that of the ECSWH-B and MSWL-B scenarios even if the electrodes and the recirculation pump were less consuming, given that in this case, the energy required by the inlet/outlet pumps was more significant.

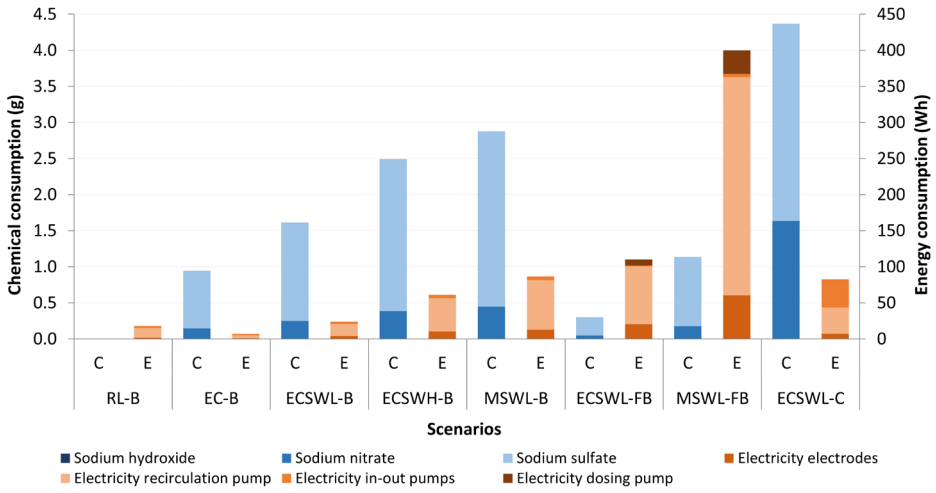

Figure 2: Chemical (C) and energy (E) consumption expressed per FU across all experimental scenarios in the vertical plate stirred tank reactor configuration. The underlying data are presented in Table A.5. The experimental conditions of the different scenarios are defined in Section 2.1.

A benchmark on the environmental profile of the different modes of operation was conducted for the vertical plate stirred tank reactor under the ECSWL-B, ECSWL-FB and ECSWL-C scenarios, since their operating conditions only differed on the batch, fed-batch and continuous type of operation, respectively. Their contributions among the selected LCA midpoint categories were calculated with respect to the highest impact value per category; hence, the relative results are depicted in Fig. 3. For all impact categories, the environmental effects of the batch operating mode were significantly lower (i.e., between 19.4% and 31.0%) with respect to the fed-batch and continuous modes due to its lower energy consumption, as shown in Fig. 2. The continuous operation was 3.5% and 14.7% lower than the fed-batch mode for the fossil resource scarcity (FRS) and freshwater eutrophication (FET) categories, respectively. In contrast, in the categories of global warming potential (GWP), terrestrial acidification (TA), marine eutrophication (ME) and terrestrial ecotoxicity (TET), the continuous operation was 2.3-63.6% higher than that of the fed-batch.

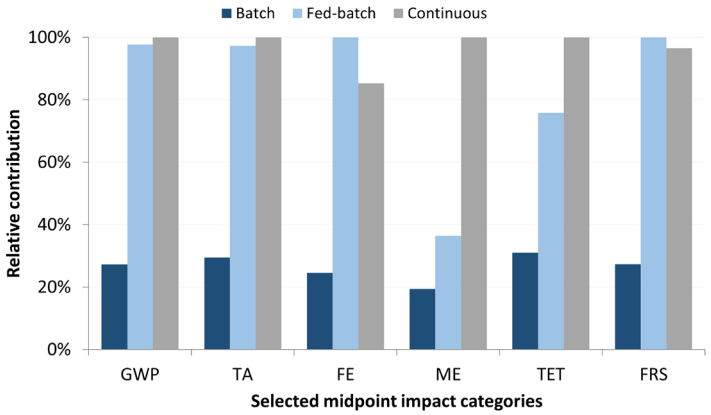

Figure 3: Environmental benchmark in the selected LCA midpoint categories for the vertical plate stirred tank reactor across equivalent scenarios operated in batch, fed-batch and continuous modes (i.e., ECSWL-B, ECSWL-FB and ECSWL-C, respectively). GWP: global warming potential, TA: terrestrial acidification, FE: freshwater eutrophication, ME: marine eutrophication, TET: terrestrial ecotoxicity, FRS: fossil resource scarcity.

Insights into the parameters contributing to each of the LCA midpoint categories are included in Fig. 4. For the batch operation (Fig. 4a), the recirculation pump accounted for most of the impact (i.e., over 53%) in all selected LCA categories, except for the terrestrial ecotoxicity (TET) and marine eutrophication (ME) categories, where sodium sulfate and sodium nitrate accounted for 35.9% and 55.9%, respectively. The impacts derived from the electricity consumed by the other pumps and the electrodes were similar across all categories, with less than a 4.1% difference. In the case of the fed-batch operation (Fig. 4b), the largest contribution was also due to the electricity consumption from the recirculation pump, which ranged from 68.6% to 72.4% on the overall impact per category. The next significant contribution was assigned to the electricity consumed by the electrodes, accounting for 17.6% to 18.5%. Apart from the electricity of the dosing pump (between 7.4-7.8%), the contribution of other process parameters in the fed-batch mode was negligible. Regarding the continuous operation (Fig. 4c), its impact distribution was similar to that of the batch operation in terms of overall energy and chemicals. The energy consumption was again the most contributing factor, where the electricity consumed by the inlet/outlet pumps and the recirculation pump were evenly distributed in all impact categories and significantly greater than that consumed by the electrodes, which accounted for a maximum of 8.5% in the freshwater eutrophication (FE) category. The predominant energy contribution in the continuous mode was only overruled in the midpoint categories of terrestrial ecotoxicity (TET) and marine eutrophication (ME), where chemicals (and particularly sodium nitrate) contributed 40.4% and 72.1%, respectively. It is also in these two categories that the continuous mode significantly surpassed the impact of the fed-batch operation (Fig. 3), which is therefore attributed to the consumption of additional chemicals. It was further evaluated that if the inlet wastewater presented higher sulfate and nitrate contents and no chemical additions were needed, the continuous operation would display an 18.7% lower environmental impact than fed-batch operation in all LCA midpoint categories. Under such hypothesis, the batch mode would correspond to an impact 76.6% lower than the fed-batch in all LCA midpoint categories.

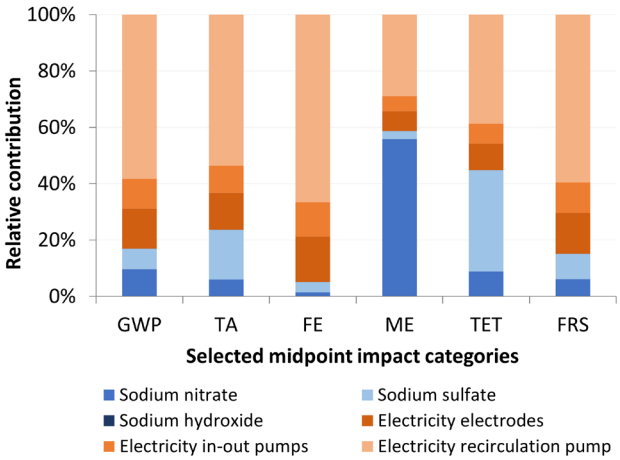

469

470 **(a)** Batch.

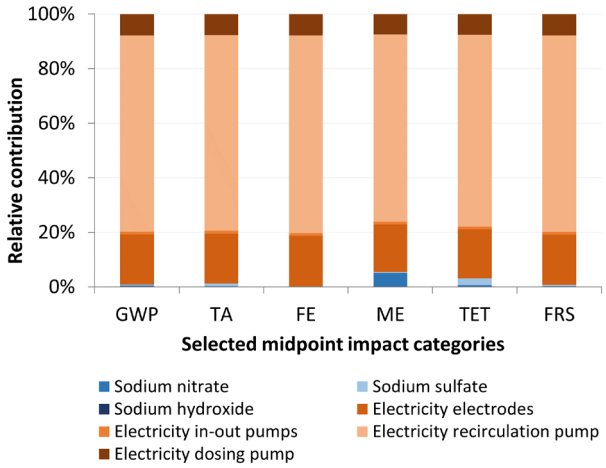

471

472 **(b)** Fed-batch.

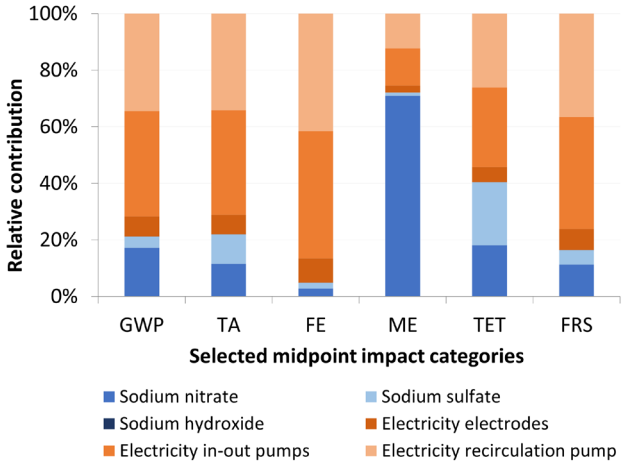

473

474 **(c)** Continuous.

475 **Figure 4:** Environmental contributions in the selected LCA midpoint categories for the vertical plate stirred tank
476 reactor in the (a) batch scenario ECSWL-B, (b) fed-batch scenario ECSWL-FB and (c) continuous scenario ECSWL-C.
477 GWP: global warming potential, TA: terrestrial acidification, FE: freshwater eutrophication, ME: marine
478 eutrophication, TET: terrestrial ecotoxicity, FRS: fossil resource scarcity.

3.2.2 Benchmark of wastewater compositions

To elucidate the environmental effects of the influent wastewater composition, the scenarios operated in batch mode (i.e., RL-B, EC-B, ECSWL-B, ECSWH-B and MSWL-B) were analysed under the standardised modular reactor configuration. Their relative contributions across the selected LCA midpoint categories are shown in Fig. 5. It can be observed that the contributions of the different scenarios are uniform across all impact categories, with the scenarios with the most complex wastewater matrices (i.e., MSWL-B and ECSWH-B) being the predominant ones. The scenarios in pure water (i.e., RL-B and EC-B) corresponded to less than 22% of the impact of the multicomponent system MSWL-B. In addition, between those two, the addition in scenario EC-B of sulfate and nitrate species above the regulatory limits contributed to an overall reduction over the RL-B scenario for all categories, except for terrestrial ecotoxicity (TET), where the relative impact was 0.1% higher. This is due to the enhanced degradation kinetics by increasing the amount of oxidative radical sources, which translates into a reduced operation time and hence a lower energy consumption (Table A.4). Nonetheless, a pure water-based operation differs from what in practice a wastewater treatment plant will be dealing with. Therefore, scenarios ECSWL-B, ECSWH-B and MSWL-B are more interesting from an implementation perspective. From their relative differences, it can be argued that increasing the wastewater matrix complexity also negatively affected the environmental profile of the treatment (i.e., an increase of 186-264% between ECSWL-B and MSWL-B in all categories), given that the more competition reactions taking place, the slower the CBZ degradation and the higher the energy consumption for the same removal target. In fact, the main contributor to the environmental impacts of these three scenarios was the electricity attributed to the recirculation pump (Fig. 6), accounting for 51-74% in the categories of global warming potential (GWP), terrestrial acidification (TA), freshwater eutrophication (FE) and fossil resource scarcity (FRS). Regarding terrestrial ecotoxicity (TET), the contribution of the recirculation pump was slightly lower, although predominant (i.e., 36-49%). Sodium nitrate was the main contributor in the marine eutrophication (ME) category, accounting for 59-62% of the overall impact.

3.2.3 Benchmark of reactor configurations

Regarding the environmental profile of the different reactor configurations in batch mode, it was observed that the vertical plate stirred tank reactor consistently presented higher LCA midpoint impact values than the standardised modular reactor (approximately 23-54% higher) regardless of the experimental scenario and the category considered (Fig. 7). An increasing trend in impact values was also observed with regard to the wastewater matrix complexity, as previously elucidated. Only the ECSWH-B and MSWL-B scenarios displayed the same impact in the marine eutrophication (ME) category for both reactors, with less than a 3% difference.

The contributions of the different categories for the vertical plate stirred tank reactor (Fig. B.6) were analogous to those mentioned above for the standardised modular reactor (Fig. 5). Therefore, the benchmark between both reactor types was conducted from an endpoint perspective, as it led to more accentuated differences among the experimental scenarios in batch mode. As depicted in Fig. 8, the single score indicator allocated to the consumption of chemicals was very similar for both reactors regardless of the scenario under consideration. In addition, its value showcased a mild increase with increasing wastewater complexity. On the

other hand, higher scores and more evident differences were found regarding energy requirements. For scenarios treating pure water matrices (i.e., RL-B and EC-B), the vertical plate stirred tank reactor scored 30-33% higher than the standardised modular reactor. As more compounds were found in the influent and hence triggered competition reactions that hindered the degradation kinetics, this difference was approximately 44-49% higher for the vertical plate stirred tank reactor, corresponding to scenarios ECSWL-B, ECSWH-B and MSWL-B.

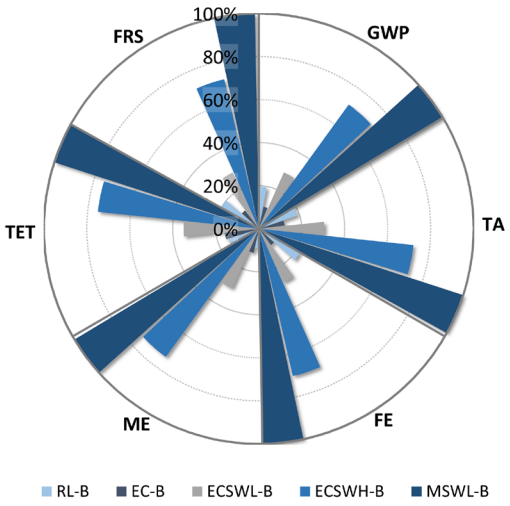

Figure 5: Environmental benchmark in the selected LCA midpoint categories for the standardised modular reactor across scenarios operated in batch mode as defined in Section 2.1. *GWP:* global warming potential, *TA*: terrestrial acidification, *FE:* freshwater eutrophication, *ME:* marine eutrophication, *TET:* terrestrial ecotoxicity, *FRS:* fossil resource scarcity.

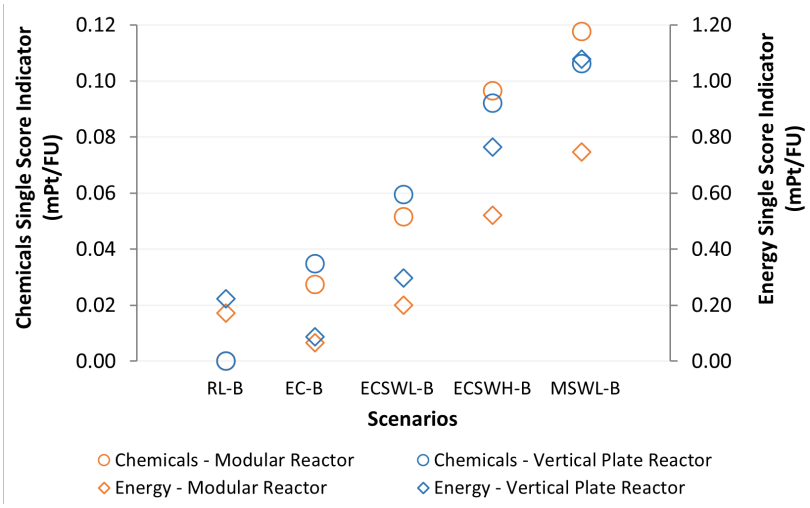

Figure 8: Single Score Indicators from LCA endpoint analysis for the standardised modular reactor and the vertical plate stirred tank reactor configurations operated in batch mode as defined in Section 2.1.

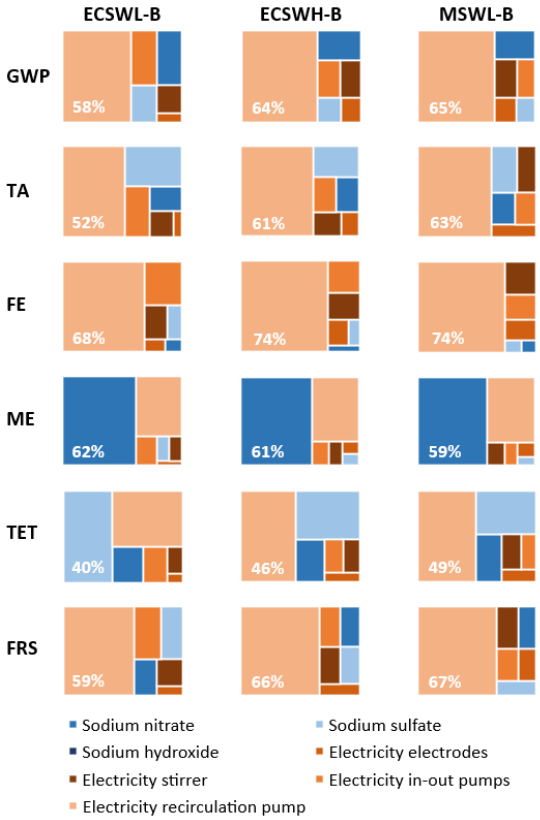

Figure 6: Environmental contributions in the selected LCA midpoint categories for the standardised modular reactor in scenarios ECSWL-B, ECSWH-B and MSWL-B as defined in Section 2.1. Data labels correspond to the contribution of the hotspot per scenario and category. *GWP:* global warming potential, *TA*: terrestrial acidification, *FE:* freshwater eutrophication, *ME:* marine eutrophication, *TET:* terrestrial ecotoxicity, *FRS:* fossil resource scarcity.

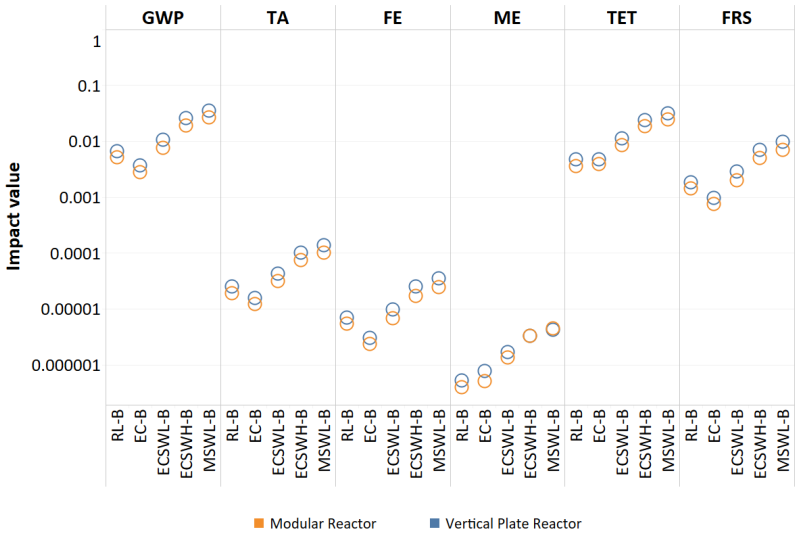

Figure 7: Environmental benchmark in the selected LCA midpoint categories for the standardised modular reactor and the vertical plate stirred tank reactor across scenarios operated in batch mode as defined in Section 2.1. GWP: global warming potential (kg CO2 eq), TA: terrestrial acidification (kg SO2 eq), FE: freshwater eutrophication (kg P eq), ME: marine eutrophication (kg N eq), TET: terrestrial ecotoxicity (kg 1,2-DCB eq), FRS: fossil resource scarcity (kg oil eq).

3.2.4 Oversizing effect

As for the standardised modular reactor configuration, the concept of oversizing effect is introduced here to account for the mismatch between the number of anodes commercially available and the number of anodes actually needed to achieve a desired CBZ removal rate. This gap occurs because this reactor configuration is composed of fixed stacks of 10 anodes, which in practice will lead the round-up in the number of anodes to the closest tenth multiple. Consequently, the energy consumption and investment costs of electrochemical treatment may also inevitably increase without being effectively exploited. The effect of oversizing was analysed for the RL-B scenario by assuming that the anodes can operate with different effective surface areas (Fig. 9). After calculating the required number of anodes for each effective surface and rounding it to the nearest tenth multiple, the number of reactors required was obtained. Depending on the differences between the theoretically required energy consumption for a given effective anode area and the actual energy consumption due to the required number of reactors (that is, the gap between the straight and the dotted lines), the oversizing may range from 0.95% to 54.3% imbalance. The smallest gap corresponded to 65% effective area, and the largest to 10%. In the case of the 90% effective anode area that was considered for scale up, a gap of 17.7% was observed.

In order to elucidate the effect of oversizing on the environmental profile of the different reactor configurations, the 17.7% intrinsic excess found in the standardised modular reactor was applied to the vertical plate stirred tank reactor. Under the EC-B scenario, a benchmark in terms of LCA midpoint and endpoint categories for the three resulting reactor configurations was conducted (Fig. 10 and Fig. 11). As shown in Fig. 10, the oversized vertical plate stirred tank reactor presented the largest contribution to all LCA midpoint categories, with a difference of 1-3% over the vertical plate stirred tank reactor and 20-36% over the standardised modular reactor. Regarding the LCA endpoint categories (Fig. 11), the scores for Human Health and Ecosystems categories were the most substantial, with the Resources category reporting scores up to 2 orders of magnitude lower. For all endpoint categories, between 63 and 72% of the individual scores were attributed to energy consumption. According to this analysis, the oversized vertical plate stirred tank reactor was again the most impactful configuration, followed closely by its non-oversized version. Similar to the outcomes of the midpoint benchmark, the 17.7% oversizing did not lead to a dramatic increase in endpoint scores, as there was a difference of approximately 2% in the Human Health and Ecosystems categories and a difference of 25% for Resources, although the latter category contributed less to the overall endpoint damage. In both the midpoint and endpoint analyses, the standardised modular reactor was the configuration with the lowest environmental impact, although inherently oversized, mainly due to the lower energy consumption of the electrodes (Table A.4) relative to the vertical plate stirred tank reactor (Table A.5). This reduction originated not only from the different anode areas involved but also from the distances between electrodes (being considerably lower for the modular reactor), which affected the calculation of the potential difference at the pilot scale (V_{diff}), as discussed in Sections 3.1.1 and 3.1.2.

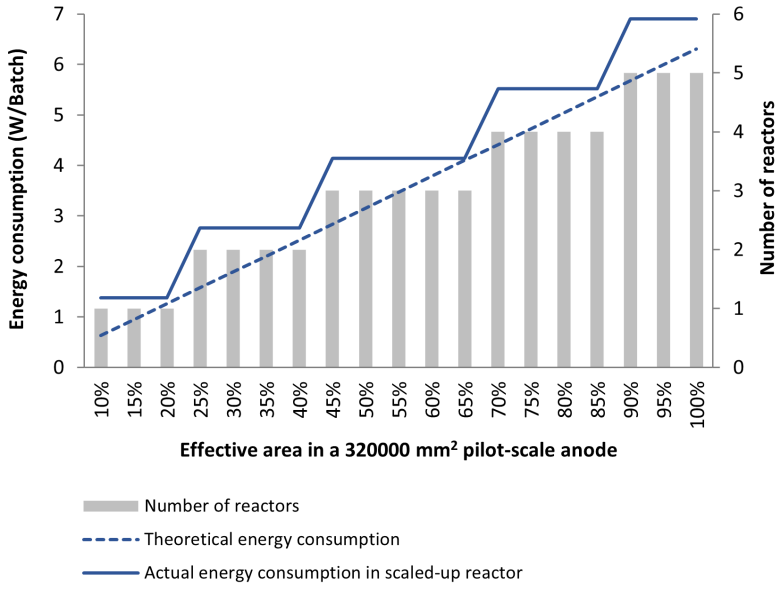

Figure 9: Correlations between energy consumption and the number of reactors with respect to the anode effective area in the RL-B scenario.

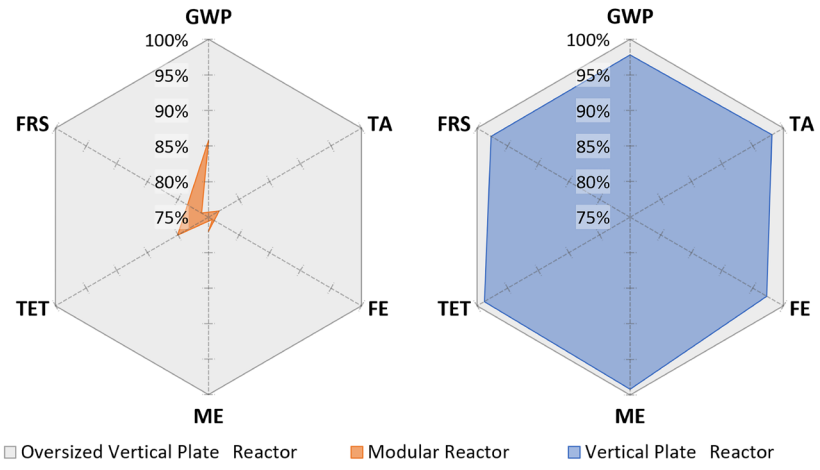

Figure 10: Environmental benchmark in the selected LCA midpoint categories for the EC-B scenario operated under different reactor configurations, including the oversizing effect. *GWP:* global warming potential, *TA*: terrestrial acidification, *FE:* freshwater eutrophication, *ME:* marine eutrophication, *TET:* terrestrial ecotoxicity, *FRS:* fossil resource scarcity.

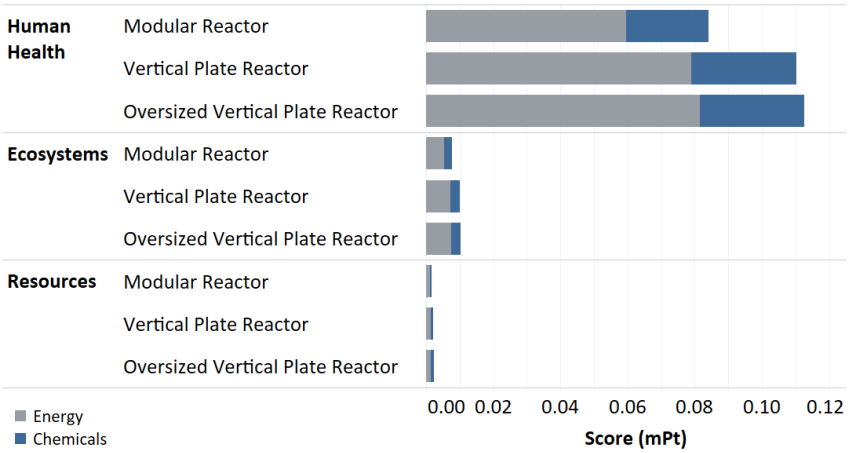

Figure 11: Environmental scores in the LCA endpoint categories for the EC-B scenario operated under different reactor configurations, including the oversizing effect.

4 Treatment selection and literature comparison

When evaluating the most sustainable mode of operation, the first finding of this work was that continuous operation showed the highest chemical consumption, given that its nitrate and sulfate requirements were above the regulatory limits, and thus, these ionic species needed to be continuously added to the wastewater influent. On the other hand, the fed-batch operation could minimise such chemical consumption with a 74-93% reduction, while the batch performance ranged in between regardless of the wastewater treated. Regarding electrical energy consumption, the fed-batch operation was the one with the highest energy demand, especially when treating wastewater with multiple pollutants. This was due not only to the energy required by the operation of the recirculation pump but also to its lower wastewater volume capacity and negatively affected degradation efficiency by competition kinetics. Energy-wise, both continuous and batch operations treating complex wastewater matrices were comparable even if the energy consumption was distributed differently across pump types. However, when the influent wastewater contained a lower content of other ions and organics, the batch operation stood out as the most environmentally friendly solution across all LCA impact categories, resulting from its lower energy consumption and regardless of the chemical additions. Therefore, from an environmental perspective, the decision-making process regarding the mode of operation comes down to the energy-related impacts, where batch is the most sustainable option, followed by continuous and fed-batch. If the addition of chemicals were to be avoided by operating with wastewater influents with enough sulfate and nitrate compositions, the batch operation would still be the leading condition, and the overall treatment would also be improved from an economic point of view.

Regarding the effect of the influent wastewater composition, it was found that targeting single vs multiple contaminant wastewater matrices significantly affected the environmental profile of the treatment, with an increase between 186-264% across the LCA impact categories considered. Here, again, these impacts derived from the negatively affected degradation efficiencies, which resulted in longer reaction times and higher energy demands by the different

pumps involved.

In this study, two different reactor types were scaled up and compared in environmental terms: a standardised modular reactor and a vertical plate stirred tank reactor. The latter presented the advantage that it allowed for a fully customisable design, as it was not restricted to the anode geometry, size or number of commercially available cell modules. Nonetheless, the vertical plate stirred tank reactor scored higher for the majority of LCA midpoint and endpoint categories, with differences up to 54% and 49%, respectively, resulting from the increased energy requirements by the electrodes and the recirculation pump. Based on complementary analysis regarding the oversizing effect, it was found that even if 17.7% was oversized, the modular reactor was the most attractive configuration.

Consequently, the most environmentally friendly configuration for the electrochemical oxidation of CBZ through BDD anodes corresponded to batch operation in a standardised modular reactor, preferably when the influent wastewater matrix had a low content of scavengers, such as other ions, organics or pollutants. The associated environmental impacts at the midpoint for these conditions are detailed in Table B.1. Despite the lack of comparable references on LCA applied to pilot-scale eAOPs for CBZ removal, a preliminary comparison of our most promising configuration in single and multicomponent systems (i.e., the ECSWL-B, ECSWH-B and MSWL-B scenarios in the standardised modular reactor) with respect to other pilot-scale treatments in terms of GWP is presented here. Given the diversity of functional units, the reported values have been extrapolated to a common reference of kg CO_2 eq per g CBZ removed (Fig. 12). Considering that the average CBZ intake for adults is 600 mg/day [60] and that approximately 72% is absorbed by the human body [8], the CO_2 emissions associated with the removal of the daily CBZ discharge per patient have been correlated to the equivalent distance covered by an average passenger car for the same environmental impact (considering that an average of 107.5 g CO_2/km was emitted in 2020 for new passenger cars registered in Europe [61]). The underlying calculations can be found in Table B.2, although it should be noted that the comparison between the studies should not be taken unquestionably, as there are considerable differences in their LCA scopes.

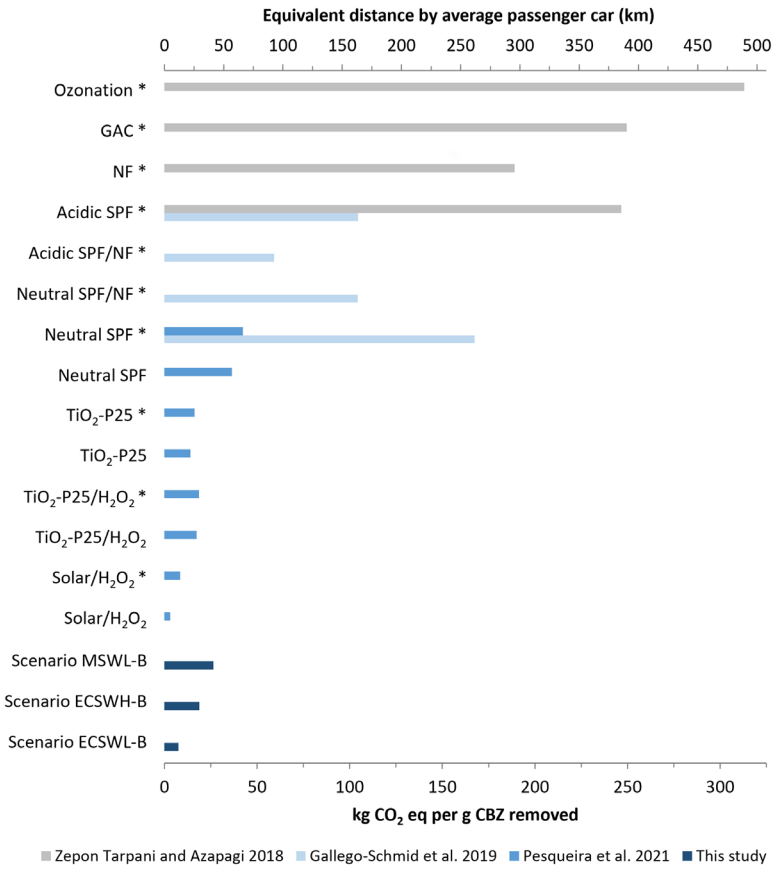

Figure 12: Reported GWP impacts (in kg CO_2 eq per g CBZ removed) for several wastewater treatments. GWP results are also linked to the equivalent distance (in km) travelled by an average passenger car for the same emissions. Treatments including the impacts associated with the infrastructure are denoted with *. *GAC:* granular activated carbon, *NF:* nanofiltration, *SPF:* solar photo-Fenton.

Pesqueira et al. (2021) conducted an LCA on pilot-scale solar-based treatments, including solar photolysis and TiO_2 photocatalysis (with and without H_2O_2 addition) and near-neutral photo-Fenton [62]. Their LCA was based on the chemical and energy consumption in the photoreactor and, at a later stage, the impact for its construction was also considered (indicated with * in Fig. 12). Solar photolysis exhibited the lowest associated GWP (i.e., 5 kg CO_2 eq per g CBZ removed excluding infrastructure), although it was argued that the applicability of the process was hindered by the lower mineralisation efficiencies attained. On the other hand, solar photo-Fenton presented the highest impact (i.e., 57 kg CO_2 eq per g CBZ removed excluding infrastructure) due to the need for acidification, neutralisation and iron removal steps. As a result, solar TiO_2-P25 treatment without H_2O_2 was presented as the most suitable alternative, considering that the catalyst should be reused at least 5 times [62]. In absolute terms, this treatment resulted in a GWP of 22 kg CO_2 eq per g CBZ removed, which increased by 15.5% when considering infrastructure impacts. In our study, the scenario that would outperform TiO_2-P25 photocatalysis would be the ECSWL-B scenario, with 7.6 kg CO_2 eq per g CBZ removed. By increasing the complexity of the wastewater matrix, the ECSWH-B and MSWL-B scenarios showed impacts of up to 18.9 and 26.5 kg CO_2 eq per g CBZ removed, respectively. However, the analysis by Pesqueira et al. (2021) did not include the impacts associated with the operation of other equipment such as pumps, which are the main sources of electricity consumption and thus

GWP. Consequently, it can be argued that our electrochemical setup entails a significantly lower environmental impact than solar photo-Fenton for the three scenarios selected, while a more comprehensive analysis of the electrical energy consumption by solar TiO_2-P25 photocatalysis is needed. Nonetheless, the electrochemical treatment has the added value of not requiring a catalyst, and therefore, avoiding the need to optimise the reuse, regeneration, operating costs and environmental impacts of the catalyst material.

Gallego-Schmid et al. (2019) evaluated several pilot-scale solar photo-Fenton (SPF) processes in combination with nanofiltration (NF). Their results showed that the NF unit helped to reduce the environmental impact of acidic and neutral SPF by 38-43% by enhancing the treatment efficiency. In terms of SPF performance, neutral SPF was hampered by the impact associated with the use of an iron complexing agent, making it less environmentally friendly than conventional acid treatment [63]. The higher impacts achieved by the neutral SPF (i.e., 167.3 kg CO_2 eq per g CBZ removed) compared to those of Pesqueira et al. (2021) could be attributed to the higher number of target pollutants (and thus process efficiency affected), the higher number of consumables (including reagents and iron complexing agents) and the inclusion of transport and dismantling in the scope. As confirmed through this study, our electrochemical treatment stands out as more sustainable, as GWP impacts are between 2.2 and 22 times lower. Zepon Tarpani and Azapagic (2018) also investigated the environmental impact of SPF, ozonation and other conventional wastewater treatments, such as granular activated carbon (GAC) and nanofiltration (NF). In terms of CBZ removal, their four treatments showed considerably higher GWP impacts than any previous work (i.e., between 189.1 and 312.9 kg CO_2 eq per g CBZ removed), presumably also due to the larger scope of the LCA [64].

In relation to previous literature on LCA applied specifically to electrochemical oxidation, the studies from Chatzisymeon et al. (2013) and Li et al. (2022) are available, although they were applied to olive mill wastewater treatment and PFAS removal from groundwater, respectively [65, 66]. In both studies, it was concluded that the environmental impact of the electrochemical treatment was primarily determined by the electrical energy consumption, which was also observed in our study. Their absolute GWP values reached 160 and 0.205 CO_2 eq per cubic metre of treated wastewater, respectively. Under the standardised modular reactor configuration, the ECSWL-B, ECSWH-B and MSWL-B scenarios presented GWP impacts of $7.6{\cdot}10^{-3}$, $1.9{\cdot}10^{-2}$ and $2.7{\cdot}10^{-2}$ kg CO_2 eq per 1 mg CBZ removed per cubic metre of treated wastewater during one day of operation. Comparison between the three assessments is certainly hampered by the different target pollutants, wastewater origins, functional units and LCA scopes considered, as reflected in the different orders of magnitude of the results obtained. Therefore, future LCA studies on electrochemical oxidation applied to the removal of pharmaceuticals are necessary to consolidate the environmental profile of eAOPs.

5 Conclusions

This study has demonstrated the importance of scaling up laboratory results for a more comprehensive evaluation of an electrochemical treatment, since most of the environmental impacts in a modelled scaled-up pilot operation were found to be related to the electrical energy

consumed by complementary pumps and not the electrochemical reactor itself. Consequently, optimising the energy requirements of all pieces of equipment is crucial to aim towards sustainable and carbon neutral wastewater treatment. In this way, the efforts made to achieve SDG No. 6 of Clean Water and Sanitation are not jeopardised by increasing the levels of CO_2 and other greenhouse gases in the atmosphere.

From an environmental point of view, this work has shown that the most promising eAOP for the removal of CBZ is carried out in a standardised modular reactor operated in batch mode, preferably when the complexity of the influent wastewater is as low as possible. Under these conditions, our eAOP has been shown to outperform previously reported AOPs, such as ozonation and solar Photo-Fenton, in terms of GWP (i.e., ranging from 10% to 96% less kg CO_2 eq per g CBZ removed). However, further LCA studies on similar eAOPs are required to confirm their suitability for future applications, especially if the scope of the LCA can be extended to a full plant operation.

Finally, it should be noted that this techno-environmental analysis is based on steady-state modelling and would therefore benefit from validation studies. To corroborate the robustness and effectiveness of the eAOP for real wastewater treatment, experiments should be replicated on a larger scale, and dynamic modelling aspects, such as possible alterations of process variables (e.g., flow rate, current density and wastewater composition) and deterioration of equipment over time (e.g., fouling of electrodes) should be evaluated. In addition, a toxicity assessment of the treated effluent is recommended to ensure safe and viable operation.

Acknowledgements

This research received funding from the European Union's EU Framework Programme for Research and Innovation H2020 under Grant Agreement No 861369 (MSCA-ETN InnovEOX), from the KU Leuven Industrial Research Council under grant number C24E/19/040 (SO4ELECTRIC), and from the HP-Nanobio project (PID2019-111163RB-I00), granted by Spanish Ministry of Science and Innovation. S. Estévez thanks the Spanish Ministry of Science, Innovation and Universities for financial support (Grant reference PRE2020-092074).

Competing interests

The authors declare no competing interests.

Supplementary Material

The Supplementary Material includes additional results regarding the scale-up modelling and environmental analyses as well as a literature review.

Author contributions

Sara Feijoo: Conceptualisation, Investigation, Validation, Visualisation, Writing - original draft, Writing - review & editing. **Sofía Estévez:** Conceptualisation, Formal analysis, Methodology, Visualisation, Writing - review & editing. **Mohammadreza Kamali:** Supervision, Writing - review & editing. **Raf Dewil:** Funding acquisition, Project administration, Supervision, Writing - review & editing. **María Teresa Moreira:** Conceptualisation, Funding acquisition, Project administration, Supervision, Writing - review & editing.

References

[1] United Nations, The Sustainable Development Goals Report 2021, https://unstats.un.org/sdgs/report/2021/The-Sustainable-Development-Goals-Report-2021.pdf (2021).

[2] D. Seibert, C. F. Zorzo, F. H. Borba, R. M. de Souza, H. B. Quesada, R. Bergamasco, A. T. Baptista, J. J. Inticher, Occurrence, statutory guideline values and removal of contaminants of emerging concern by Electrochemical Advanced Oxidation Processes: A review, Sci. Total Environ. 748 (2020) 141527. doi:10.1016/j.scitotenv.2020.141527.

[3] N. H. Tran, M. Reinhard, K. Y.-H. Gin, Occurrence and fate of emerging contaminants in municipal wastewater treatment plants from different geographical regions - A review, Water Res. 133 (2018) 182–207. doi:10.1016/j.watres.2017.12.029.

[4] X. E. Hu, X. Luo, G. Xiao, Q. Yu, Y. Cui, G. Zhang, R. Zhang, Y. Liu, Y. Zhou, Z. Zeng, Low-cost novel silica@ polyacrylamide composites: fabrication, characterization, and adsorption behavior for cadmium ion in aqueous solution, Adsorption 26 (7) (2020) 1051–1062. doi:10.1007/s10450-020-00225-4.

[5] T. Lu, H. Liang, W. Cao, Y. Deng, Q. Qu, W. Ma, R. Xiong, C. Huang, Blow-spun nanofibrous composite self-cleaning membrane for enhanced purification of oily wastewater, J. Colloid Interface Sci. 608 (2022) 2860–2869. doi:10.1016/j.jcis.2021.11.017.

[6] T. Hata, H. Shintate, S. Kawai, H. Okamura, T. Nishida, Elimination of carbamazepine by repeated treatment with laccase in the presence of 1-hydroxybenzotriazole, J. Hazard. Mater. 181 (1) (2010) 1175–1178. doi:10.1016/j.jhazmat.2010.05.103.

[7] Y. Zhang, S.-U. Geißen, In vitro degradation of carbamazepine and diclofenac by crude lignin peroxidase, J. Hazard. Mater. 176 (1) (2010) 1089–1092. doi:10.1016/j.jhazmat.2009.10.133.

[8] Y. Zhang, S.-U. Geißen, C. Gal, Carbamazepine and diclofenac: Removal in wastewater treatment plants and occurrence in water bodies, Chemosphere 73 (8) (2008) 1151–1161. doi:10.1016/j.chemosphere.2008.07.086.

[9] J. L. Wilkinson, A. B. A. Boxall, D. W. Kolpin, K. M. Y. Leung, R. W. S. Lai, C. Galbán-Malagón, A. D. Adell, J. Mondon, M. Metian, R. A. Marchant, A. Bouzas-Monroy, A. Cuni-Sanchez, A. Coors, P. Carriquiriborde, M. Rojo, C. Gordon, M. Cara, M. Moermond, T. Luarte, V. Petrosyan, Y. Perikhanyan, C. S. Mahon, C. J. McGurk, T. Hofmann, T. Kormoker, V. Iniguez, J. Guzman-Otazo, J. L. Tavares, F. G. D. Figueiredo, M. T. P. Razzolini, V. Dougnon, G. Gbaguidi, O. Traoré, J. M. Blais, L. E. Kimpe, M. Wong, D. Wong, R. Ntchantcho, J. Pizarro, G.-G. Ying, C.-E. Chen, M. Páez, J. Martínez-Lara, J.-P. Otamonga, J. Poté, S. A. Ifo, P. Wilson, S. Echeverría-Sáenz, N. Udikovic-Kolic, M. Milakovic, D. Fatta-Kassinos, L. Ioannou-Ttofa, V. Belusová, J. Vymazal, M. Cárdenas-Bustamante, B. A. Kassa, J. Garric, A. Chaumot, P. Gibba, I. Kunchulia, S. Seidensticker, G. Lyberatos, H. P. Halld'orsson, M. Melling, T. Shashidhar, M. Lamba, A. Nastiti, A. Supriatin, N. Pourang, A. Abedini, O. Abdullah, S. S. Gharbia, F. Pilla, B. Chefetz, T. Topaz, K. M. Yao, B. Aubakirova, R. Beisenova, L. Olaka, J. K. Mulu, P. Chatanga, V. Ntuli, N. T. Blama, S. Sherif, A. Z. Aris, L. J. Looi, M. Niang, S. T. Traore, R. Oldenkamp, O. Ogunbanwo, M. Ashfaq, M. Iqbal, Z. Abdeen, A. O'Dea, J. M. Morales-Saldañaa, M. Custodio, H. de la Cruz, I. Navarrete, F. Carvalho, A. B. Gogra, B. M. Koroma, V. Cerkvenik-Flajs, M. Gombac, M. Thwala, K. Choi, H. Kang, J. L. C. Ladu, A. Rico, P. Amerasinghe, A. Sobek, G. Horlitz, A. K. Zenker, A. C. King, J.-J. Jiang, R. Kariuki, M. Tumbo, U. Tezel, T. T. Onay, J. B. Lejju, Y. Vystavna, Y. Vergeles, H. Heinzen, A. Pérez-Parada, D. B. Sims, M. Figy, D. Good, C. Teta, Pharmaceutical pollution of the world's rivers, PNAS 119 (8) (2022). doi:10.1073/pnas.2113947119.

[10] R. Dewil, D. Mantzavinos, I. Poulios, M. A. Rodrigo, New perspectives for Advanced Oxidation Processes, J. Environ. Manage. 195 (2017) 93–99. doi:10.1016/j.jenvman.2017.04.010.

[11] L. Feng, E. D. van Hullebusch, M. A. Rodrigo, G. Esposito, M. A. Oturan, Removal of residual anti-inflammatory and analgesic pharmaceuticals from aqueous systems by electrochemical advanced oxidation processes. A review, Chem. Eng. J. 228 (2013) 944–964. doi:10.1016/j.cej.2013.05.061.

[12] I. Sirés, E. Brillas, M. A. Oturan, M. A. Rodrigo, M. Panizza, Electrochemical Advanced Oxidation Processes: Today and tomorrow. A review, Environ. Sci. Pollut. Res. 21 (2014) 8336–8367. doi:10.1007/s11356-014-2783-1.

[13] S. Garcia-Segura, J. D. Ocon, M. N. Chong, Electrochemical oxidation remediation of real wastewater effluents - A review, Process Saf. Environ. Prot. 113 (2018) 48–67. doi:10.1016/j.psep.2017.09.014.

[14] C. A. Martínez-Huitle, S. Ferro, Electrochemical oxidation of organic pollutants for the wastewater treatment: Direct and indirect processes, Chem. Soc. Rev. 35 (12) (2006) 1324–1340. doi:10.1039/B517632H.

[15] J. Radjenovic, D. L. Sedlak, Challenges and Opportunities for Electrochemical Processes as Next-Generation Technologies for the Treatment of Contaminated Water, Environ. Sci. Technol. 49 (19) (2015) 11292–11302. doi:10.1021/acs.est.5b02414.

[16] S. Garcia-Segura, J. Keller, E. Brillas, J. Radjenovic, Removal of organic contaminants from secondary effluent by anodic oxidation with a boron-doped diamond anode as tertiary treatment, J. Hazard. Mater. 283 (2015) 551–557. doi:10.1016/j.jhazmat.2014.10.003.

[17] G. Divyapriya, P. Nidheesh, Electrochemically generated sulfate radicals by boron doped diamond and its environmental applications, Curr. Opin. Solid State Mater Sci. 25 (3) (2021) 100921. doi:10.1016/j.cossms.2021.100921.

[18] S. O. Ganiyu, C. A. Martínez-Huitle, M. A. Oturan, Electrochemical advanced oxidation processes for wastewater treatment: Advances in formation and detection of reactive species and mechanisms, Curr. Opin. Electrochem. 27 (2021) 100678. doi:10.1016/j.coelec.2020.100678.

[19] H. Song, L. Yan, J. Jiang, J. Ma, Z. Zhang, J. Zhang, P. Liu, T. Yang, Electrochemical activation of persulfates at BDD anode: Radical or nonradical oxidation?, Water Res. 128 (2018) 393–401. doi:10.1016/j.watres.2017.10.018.

[20] X. Yu, M. Zhou, Y. Hu, K. Groenen Serrano, F. Yu, Recent updates on electrochemical degradation of bio-refractory organic pollutants using BDD anode: a mini review, Environ. Sci. Pollut. Res. 21 (14) (2014) 8417–8431.

[21] K. Groenen-Serrano, E. Weiss-Hortala, A. Savall, P. Spiteri, Role of hydroxyl radicals during the competitive electrooxidation of organic compounds on a boron-doped diamond anode, Electrocatalysis 4 (4) (2013) 346–352.

[22] L. Chen, C. Lei, Z. Li, B. Yang, X. Zhang, L. Lei, Electrochemical activation of sulfate by BDD anode in basic medium for efficient removal of organic pollutants, Chemosphere 210 (2018) 516–523. doi:10.1016/j.chemosphere.2018.07.043.

[23] Y.-U. Shin, H.-Y. Yoo, Y.-Y. Ahn, M. S. Kim, K. Lee, S. Yu, C. Lee, K. Cho, H. il Kim, J. Lee, Electrochemical oxidation of organics in sulfate solutions on boron-doped diamond electrode: Multiple pathways for sulfate radical generation, Appl. Catal. B: Environm. 254 (2019) 156–165. doi:10.1016/j.apcatb.2019.04.060.

[24] C. T. Benatti, C. R. G. Tavares, E. Lenzi, Sulfate removal from waste chemicals by precipitation, J. Environ. Manage. 90 (1) (2009) 504–511. doi:10.1016/j.jenvman.2007.12.006.

[25] A. Sarti, M. Zaiat, Anaerobic treatment of sulfate-rich wastewater in an anaerobic sequential batch reactor (AnSBR) using butanol as the carbon source, J. Environ. Manage. 92 (6) (2011) 1537–1541. doi:10.1016/j.jenvman.2011.01.009.

[26] S. Feijoo, M. Kamali, R. Dewil, Effects of wastewater composition and reactor operating mode on the removal of micropollutants via electrochemical advanced oxidation, J. Water Process. Eng. 50 (2022) 103220. doi:10.1016/j.jwpe.2022.103220.

[27] H. Wang, Y. Yang, A. A. Keller, X. Li, S. Feng, Y.-N. Dong, F. Li, Comparative analysis of energy intensity and carbon emissions in wastewater treatment in USA, Germany, China and South Africa, Appl. Energ. 184 (2016) 873–881. doi:10.1016/j.apenergy.2016.07.061.

[28] P. Zawartka, D. Burchart-Korol, A. Blaut, Model of carbon footprint assessment for the life cycle of the system of wastewater collection, transport and treatment, Sci. Rep. 10 (2020) 5799. doi:10.1038/s41598-020-62798-y.

[29] M. Maktabifard, E. Zaborowska, J. Makinia, Energy neutrality versus carbon footprint minimization in municipal wastewater treatment plants, Bioresour. Technol. 300 (2020) 122647. doi:10.1016/j.biortech.2019.122647.

[30] European Commission, Council Directive of 12 December 1991 concerning the protection of waters against pollution caused by nitrates from agricultural sources (91/676/EEC), http://data.europa.eu/eli/dir/1991/676/2008-12-11 (2022).

[31] European Commission, Council Directive of 3 November 1998 on the quality of water intended for human consumption (98/83/EC), http://data.europa.eu/eli/dir/1998/83/oj (2022).

[32] A. Anglada, A. Urtiaga, I. Ortiz, Pilot Scale Performance of the Electro-Oxidation of Landfill Leachate at Boron-Doped Diamond Anodes, Environ. Sci. Technol. 43 (6) (2009) 2035–2040. doi:10.1021/es802748c.

[33] A. Dominguez-Ramos, A. Irabien, Analysis and modeling of the continuous electro-oxidation process for organic matter removal in urban wastewater treatment, Ind. Eng. Chem. Res. 52 (22) (2013) 7534–7540. doi:10.1021/ie303021v.

[34] A. Urtiaga, P. Gómez, A. Arruti, I. Ortiz, Electrochemical removal of tetrahydrofuran from industrial wastewaters: anode selection and process scale-up, J. Chem. Technol. Biotechnol. 89 (8) (2014) 1243–1250. doi:10.1002/jctb.4384.

[35] A. Cano, C. Barrera, S. Cotillas, J. Llanos, P. Cañizares, M. A. Rodrigo, Use of DiaCell modules for the electro-disinfection of secondary-treated wastewater with diamond anodes, Chem. Eng. J. 306 (2016) 433–440. doi:10.1016/j.cej.2016.07.090.

[36] F. Souza, C. Sáez, M. Lanza, P. Cañizares, M. A. Rodrigo, Towards the scale-up of electrolysis with diamond anodes: effect of stacking on the electrochemical oxidation of 2,4 D, J. Chem. Technol. Biotechnol. 91 (3) (2016) 742–747. doi:10.1002/jctb.4639.

[37] S. G. Xu, Modeling and Experimental Study of Electrochemical Oxidation of Organics on Boron-Doped Diamond Anode, CNL Nucl. Rev. 7 (1) (2018) 103–117. doi:10.12943/CNR.2016.00018.

[38] C. A. Martínez-Huitle, E. Brillas, A critical review over the electrochemical disinfection of bacteria in synthetic and real wastewaters using a boron-doped diamond anode, Curr. Opin. Solid State Mater. Sci. 25 (4) (2021) 100926. doi:10.1016/j.cossms.2021.100926.

[39] O. M. Cornejo, M. F. Murrieta, L. F. Castañeda, J. L. Nava, Characterization of the reaction environment in flow reactors fitted with BDD electrodes for use in electrochemical advanced oxidation processes: A critical review, Electrochim. Acta 331 (2020) 135373. doi:10.1016/j.electacta.2019.135373.

[40] O. M. Cornejo, M. F. Murrieta, L. F. Castañeda, J. L. Nava, Electrochemical reactors equipped with BDD electrodes: Geometrical aspects and applications in water treatment, Curr. Opin. Solid State Mater. Sci. 25 (4) (2021) 100935. doi:10.1016/j.cossms.2021.100935.

[41] M. A. Sandoval, W. Calzadilla, R. Salazar, Influence of reactor design on the electrochemical oxidation and disinfection of wastewaters using boron-doped diamond electrodes, Curr. Opin. Electrochem. 33 (2022) 100939. doi:10.1016/j.coelec.2022.100939.

[42] T. Muddemann, D. Haupt, M. Sievers, U. Kunz, Electrochemical reactors for wastewater treatment, ChemBioEng Rev. 6 (5) (2019) 142–156. doi:10.1002/cben.201900021.

[43] L. F. Arenas, C. P. de León, F. C. Walsh, Critical review—the versatile plane parallel electrode geometry: An illustrated review, J. Electrochem. Soc. 167 (2) (2020) 023504. doi:10.1149/1945-7111/ab64ba.

[44] A. Urtiaga, P. Fernandez-Castro, P. Gómez, I. Ortiz, Remediation of wastewaters containing tetrahydrofuran. Study of the electrochemical mineralization on BDD electrodes, Chem. Eng. J. 239 (2014) 341–350. doi:10.1016/j.cej.2013.11.028.

[45] F. Walsh, P. Trinidad, D. Gilroy, Conversion Expressions for Electrochemical Reactors which Operate under Mass Transport Controlled Reaction Conditions – Part II: Batch Recycle, Cascade and Recycle Loop Reactors, Int. J. Engng Ed. 21 (5) (2005) 981–992.

[46] M. Panizza, P. Michaud, G. Cerisola, C. Comninellis, Anodic oxidation of 2-naphthol at boron-doped diamond electrodes, J. Electroanal. Chem. 507 (1-2) (2001) 206–214.

[47] Ángela Anglada, A. M. Urtiaga, I. Ortiz, Laboratory and pilot plant scale study on the electrochemical oxidation of landfill leachate, J. Hazard. Mater. 181 (1) (2010) 729–735. doi:10.1016/j.jhazmat.2010.05.073.

[48] Speroni S.p.A., Speroni Water Pumps - General Catalogue, https://www.speroni.it/pub/media/cataloghi/SPERONI%20cat.Gen.2018%2060hz%20rev2.pdf (2018).

[49] J. Santos, V. Geraldes, S. Velizarov, J. Crespo, Characterization of fluid dynamics and mass-transfer in an electrochemical oxidation cell by experimental and CFD studies, Chem. Eng. J. 157 (2) (2010) 379–392. doi:10.1016/j.cej.2009.11.021.

[50] Redox.me, Peristaltic pump, model A, https://redox.me/products/peristaltic-pump-model-a-0-07-380-ml-per-min (2021).

[51] Golander Pump, WT600F-65 Intelligent Dispensing Peristaltic Pump, https://www.golanderpump.com/wt600f-65-intelligent-dispensing-peristaltic-pump.html (2021).

[52] International Organization for Standardization, ISO 14040:2006. Environmental management – Life cycle assessment – Principles and framework, https://www.iso.org/standard/37456.html (2006).

[53] International Organization for Standardization, ISO 14044:2006. Environmental management – Life cycle assessment – Requirements and guidelines,

https://www.iso.org/standard/38498.html (2006).

[54] National Institute for Public Health and the Environment (The Netherlands), ReCiPe 2016 v1.1 - A harmonized life cycle impact assessment method at midpoint and endpoint level, https://www.rivm.nl/en/life-cycle-assessment-lca/recipe (2016).

[55] PRé Sustainability B.V., SimaPro 9.3., https://simapro.com/wp-content/uploads/2021/12/FullUpdateInstructionsToSimaPro930.pdf (2021).

[56] D. Antoniou, A. Tzimas, S. M. Rowland, Transition from alternating current to direct current low voltage distribution networks, IET Gener. Transm. Distrib. 9 (12) (2015) 1391– 1401. doi:10.1049/iet-gtd.2014.0823.

[57] Michelet Dorceus, Cell Culture Scale-Up in Stirred-TankvSingle-Use Bioreactors, https://www.eppendorf.com/product-media/doc/en/633183/Fermēntors- Biōreactors Publication BioBLU-c Cell-Culture-Scale-Up-BioBLU-Single-Vessels.pdf (2018).

[58] V. Schlüter, W.-D. Deckwer, Gas/liquid mass transfer in stirred vessels, Chem. Eng. Sci. 47 (9) (1992) 2357–2362. doi:10.1016/0009-2509(92)87060-4.

[59] S. Başbuğ, G. Papadakis, J. C. Vassilicos, DNS investigation of the dynamical behaviour of trailing vortices in unbaffled stirred vessels at transitional Reynolds numbers, Phys. Fluids 29 (6) (2017). doi:10.1063/1.4983494.

[60] G. Grześk, W. Stolarek, M. Kasprzak, E. Grześk, D. Rogowicz, M. Wiciński, M. Krzyżanowski, Therapeutic Drug Monitoring of Carbamazepine: A 20-Year Observational Study, J. Clin. Med. 10 (22) (2021). doi:10.3390/jcm10225396.

[61] European Environmental Agency, CO_2 performance of new passenger cars in Europe, https://www.eea.europa.eu/ims/co2-performance-of-new-passenger (2022).

[62] J. F. Pesqueira, M. F. R. Pereira, A. M. Silva, A life cycle assessment of solar-based treatments (H_2O_2, TiO_2 photocatalysis, circumneutral photo-Fenton) for the removal of organic micropollutants, Sci. Total Environ. 761 (2021) 143258. doi:10.1016/j.scitotenv.2020.143258.

[63] A. Gallego-Schmid, R. R. Z. Tarpani, S. Miralles-Cuevas, A. Cabrera-Reina, S. Malato, A. Azapagic, Environmental assessment of solar photo-Fenton processes in combination with nanofiltration for the removal of micro-contaminants from real wastewaters, Sci. Total Environ. 650 (2019) 2210–2220. doi:10.1016/j.scitotenv.2018.09.361.

[64] R. R. Zepon Tarpani, A. Azapagic, Life cycle environmental impacts of advanced wastewater treatment techniques for removal of pharmaceuticals and personal care products (PPCPs), J. Environ. Manage. 215 (2018) 258–272. doi:10.1016/j.jenvman.2018.03.047.

[65] E. Chatzisymeon, S. Foteinis, D. Mantzavinos, T. Tsoutsos, Life cycle assessment of advanced oxidation processes for olive mill wastewater treatment, J. Clean. Prod. 54 (2013)

965 229–234. doi:10.1016/j.jclepro.2013.05.013.

966 [66] G. Li, J. Dunlap, Y. Wang, Q. Huang, K. Li, Environmental Life Cycle Assessment (LCA) of
967 Treating PFASs with Ion Exchange and Electrochemical Oxidation Technology, ACS ES&T Water
968 2 (9) (2022) 1555–1564. doi:10.1021/acsestwater.2c00196.